

*Original article*

CHARACTERIZATION OF HISTORICAL MORTAR USED IN LOOM  
FACTORY SITE AT ABYDOS

Osman, A.<sup>1</sup>, Bartz, W.<sup>2</sup> & Kosciuk, J.<sup>3</sup>

<sup>1</sup> Conservation dept., Faculty of Archaeology, Sohag Univ., Sohag,, Egypt.

<sup>2</sup> Institute of Geological Sciences, Wroclaw Univ., Wroclaw, Poland.

<sup>3</sup> History of Architecture, Arts and Technology dept., Wroclaw Univ. of Technology, Wroclaw, Poland.

E-mail: [amrosman75@gmail.com](mailto:amrosman75@gmail.com)

Received 3/7/2016

Accepted 13/12/2016

**Abstract**

*This paper aims to characterize historical mortars taken from joints in Loom Factory site at Abydos Sohag (Egypt). This characterization includes their composition and technology, their state of preservation as well as provides a guide for their possible conservation process. A multidisciplinary approach has been adopted for investigations. Samples were investigated by means of visual inspection, polarizing microscope (PM), scanning electron microscope (SEM) coupled with energy dispersive X-ray unit (EDX), powder X-ray diffraction (XRD), hydrochloric acid (HCl) attack, sieving analysis, deferential thermal analysis (DTA-TG) and physical tests. Obtained results allowed to fully characterize mineralogical, chemical, and mechanical properties of selected mortar samples. They show a similarity of type, and binder/aggregate ratio. This similarity can be attributed to one building phase using the same source of materials.*

**Keywords:** *Abydos, Loom factory, Mortar, Characterization.*

**1. Introduction**

Loom Factory is located at Araba al-Madfuna, about one kilometer to the south of the famous temple of Seti I in Abydos and about 47 km to the south of Sohag (coordinates: 26°10'41.28"N; 31°55'39.92"E). First excavations at that site were done on February 1977 by the Egyptian Department of Antiquities. The investigated area measures 700 meters (E-W) and 60 meters (N-S) [1]. According to excavators, it can be only roughly dated back to the late roman

and Byzantine period. The main complex of our interest is a small Byzantine loom factory consisting of medium sized peristyle, and a large hall attached to it. According to Farrag, (1983) [1] a full description of that site including the thickness of the walls and applied materials was given. No other additional information about this place exist in literature, except a paper mentioned the use of pit looms at that site and described them as a treadle pit [2].

## 2. Materials & Methods

Since the building is relatively small, only few representative samples were taken from different remnants of walls at four locations, which are still visible on the site. All samples represent jointing mortars and were carefully taken with use of hammer and chisel, from the western and southern walls of building and from the unearthed two loom pits. The map of the excavated site and locations of samples are presented in fig. (1-a, b) & fig. (2-a, b, c, d). These samples have been prepared to be investigated by the naked eye in terms of color, state of preservation, and visible aggregates. Thickness of samples was measured already in situ and rechecked once more in the laboratory using digital calliper. In addition, polished sections (ca. 45  $\mu\text{m}$  thick) were observed by use of a stereomicroscope Zeiss STEMI 2000-C equipped with digital camera Canon Powershot G10. Thin sections of intact piece of each location were prepared in a similar way, but with thinner slices (thickness of ca. 30  $\mu\text{m}$ ) for petrographic analysis [3]. They were examined with transmitted light polarizing microscope (Zeiss Axiolab Opton) equipped with Canon Powershot G2 digital camera coupled to the microscope through an eyepiece adapter. Few grams of each sample, bulk as well as sieved (0.063 mm) and enriched in binder one [4, 5] were prepared for powder X-ray diffraction analysis. Both groups of samples were analyzed with Siemens D 5005 powder diffractometer, using  $\text{CoK}\alpha$  radiation, at scanning speed  $2\theta=2.0^\circ/\text{min}$  and 30 kV, 20 mA current [6]. Different mineralogical phases were identified using PANalytical X'pert high score plus software. For microstructural analysis, samples were examined by scanning electron microscope SEM-VEGA LSU TESCAN, which was equipped with an X-ray detector (EDX) (Oxford Inca-pentaFETX3 detector). Binder/aggregate

ratio was calculated by separating visible particles of lime lumps or carbonaceous aggregates manually under stereomicroscope, then by dissolving the rest of sample in diluted HCl acid (2 Mol. HCl) to separate insoluble aggregates from the binder. Then, insoluble residue was extracted and washed many times until pH value of solutions was neutral (pH=7). Then, they were dried and weighed until they reached constant weight. Finally, the particle size distribution of insoluble fractions was determined using dry sieving. The remaining filtrate containing soluble elements was chemically investigated by means of atomic absorption spectroscopy (AAS) [7]. The quantitative analysis of soluble elements was done using a flame atomic absorption Spectro-meter (FAAS) Avanta Sigma GBC including elements Ca, Fe, Si, Al, Mg, Mn, K, Na and Ti. Those elements were converted into oxides before cementation index (CI) was calculated, according to the equation proposed by Boynton [8]. In addition, the amount of  $\text{Cl}^-$  ions and  $\text{SO}_3^{-2}$  were determined using a colorimetric method [9]. Differential thermal analysis (DTA) and simultaneous thermo-gravimetric analysis (TG) were carried out with apparatus NETZSCH STA 409 Pc/Luxx with crucible  $\text{Al}_2\text{O}_3$  in nitrogen atmosphere ( $\text{N}_2$ ) in the temperature range 40  $^\circ\text{C}$  - 1000  $^\circ\text{C}$ , with the heating rate 10  $^\circ\text{C}/\text{min}$ . Mass loss of samples at certain temperatures was determined, allowing us to calculate amount of carbonates [10]. Physical properties of samples such as moisture content, density, and porosity were measured. Porosity was measured using Gas Pycnometer AccuPyc<sup>TM</sup> [11]. 1330. For compressive strength tests, samples were prepared by adding two bars for the irregular samples [12-14] and tested by device machine MTS 858 Mini Bionix.

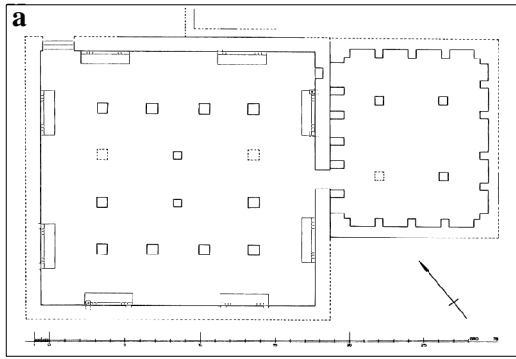


Figure (1) Shows **a.** plan of the loom factory site (After Farag, 1983), **b.** general view of the site.



Figure (2) Shows locations of samples **a.** AN1 the southern wall of the site, **b.** AN2 from the western wall of the site, **c.** AN3 from 1<sup>st</sup> loom pit, **d.** AN4 from 2<sup>nd</sup> loom

### 3. Results

#### 3.1. Visual examination results

Results of examination by naked eye and stereomicroscope revealed similarity between all samples in terms of grayish color, presence of various and distinct components such as charcoal, lime lumps, organic matters, and brick fragments. All of them represent also relatively good state of preservation. Thickness of all samples is similar ranging from 20.2 mm for sample AN2

that belong to the western wall of the site, up to 23.0 mm for sample AN4 belonging to a wall of one of the loom pits. Small amount of quartz grains was observed in all samples. The investigation results of the studied samples by naked eye and stereomicroscope are summarized in tab. (1). In addition, the samples' features and their polished sections are shown in fig. (3-a, b, c, d).

Table (1). Results of visual examination of jointing mortar samples

Samples' locations	Color	Thickness Avg. (mm)	Charcoal	Brick fragments	Lime lumps	Organic materials	State of preservation
AN1	Grayish	21.6	++	+	++	+	Coherent
AN2		20.2	++	+	++	+	
AN3		22.5	++	+	+	+	
AN4		23.0	++	+	+++	++	
		(+++) <i>Very abundant</i>	(++) <i>Abundant</i>			(+) <i>Rare</i>	(-) <i>Not present</i>

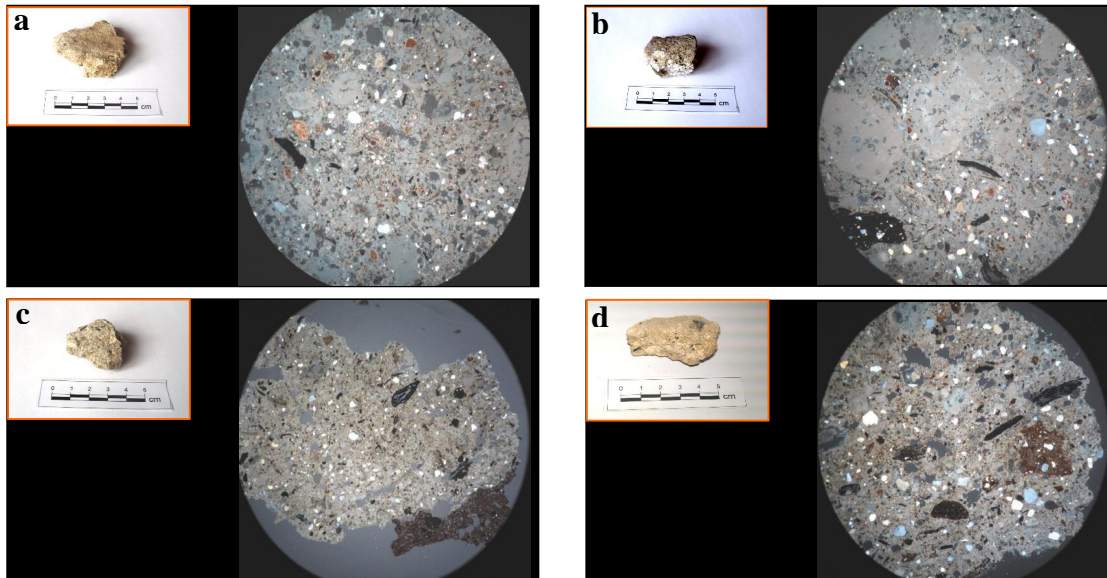


Figure (3) Shows **a.** sample AN1 from the southern wall (on the left) and photomicrograph of polished section (on the right) showing presence of lime lumps and few small brick fragments, **b.** sample AN2 from the western wall of the site and photomicrograph of polished section showing big lime lumps as well as presence of charcoal pieces, **c.** sample AN3 from the 1<sup>st</sup> loom pit (on the left) and photomicrograph of polished section (on the right) showing small amount of quartz, **d.** sample AN4 from the 2<sup>nd</sup> loom pit (on the left) and photomicrograph of polished section (on the right) showing presence of quartz grains, charcoal pieces as well as rather big fragment of red brick.

### 3.2. Petrographic results

The results of the petrographic analysis revealed similar mineralogical components for all samples, including rounded quartz grains as major constituent of their aggregate. Some of them were thermally transformed, strongly cracked, healed and surrounded with thin silica glass film. This feature is typical for sample AN1 that belongs to the southern wall. In addition, angular fragments of limestone and abundant amount of large lime lumps were identified, reaching up to 4 mm in diameter, fig. (4-a). Brick fragments are less abundant, but occurring as a subordinate constituent in all samples. Binding mass is not homogenous consisting of micrite as well as lime lumps. Charcoal is present and characteristic for sample AN1, while fresh (i.e.

not pyrolyzed) organic matter (with well visible structure of wood) is less abundant. Cracks within the binder filled with secondary weathering product (gypsum) were also observed. Uncommon poly-crystalline grains of calcite were observed in sample AN2, fig. (4-b). Some of them are partly calcined; their primary carbonate crystals are replaced by micrite. In addition, the presence of some other lithic grains of various rocks such as granodiorite, and siliceous sedimentary rock (cherts) were identified. Sample AN3, fig. (4-c) differs a little in comparison to other samples, being depleted in limestone fragments and lime lumps showing blurred boundaries with surrounding binder mass. As accessory minerals amphibole, garnet, K-feldspars

(perthite, microcline), plagioclase, glauconite and epidote were found in sample AN1. In addition, sparse biotite, which is strongly weathered to secondary chlorite was detected, as for sample AN2, amphibole, zircon, pyroxene, feldspars,

and epidote were detected, while sample AN3 show amphibole; plagioclase, weathered glauconite as well as fragment of volcanic rock. Biotite, K-feldspars, epidote plagioclase, and amphibole were identified in sample AN4, fig. (4-d).

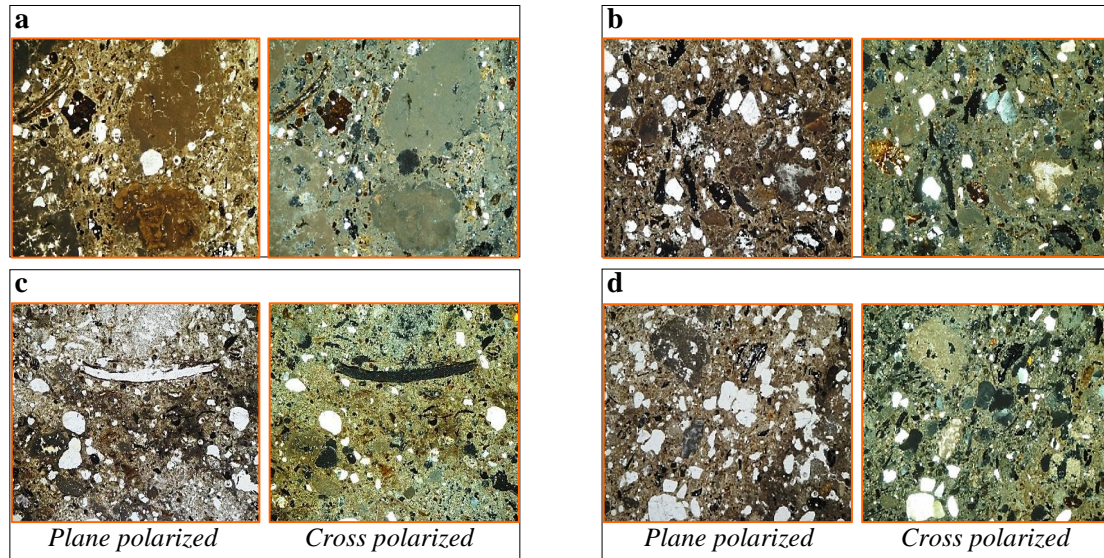


Figure (4) Shows thin section micrographs under *plane polarized* (left) & *cross polarized* (right): Field of view is ca. 6 mm **a.** sample AN1 Lime lumps up to 4 mm, **b.** sample AN2, **c.** sample AN3, **d.** sample AN4

### 3.3. Results of powder X-ray diffraction

X-ray diffraction results of both bulk and binder samples are showed in, fig. (5-a, b, c, d). For bulk samples (AN1, AN3), obtained results revealed calcite and quartz are the two main phases. Vaterite and halite are present as minor phases. The second group i.e.

mortars AN1 and AN3 enriched in binder revealed calcite and vaterite as main phases in both samples. Small amount of quartz was present as remnants of sieving in both samples. In case of binder fraction of sample AN3, aragonite was detected too.

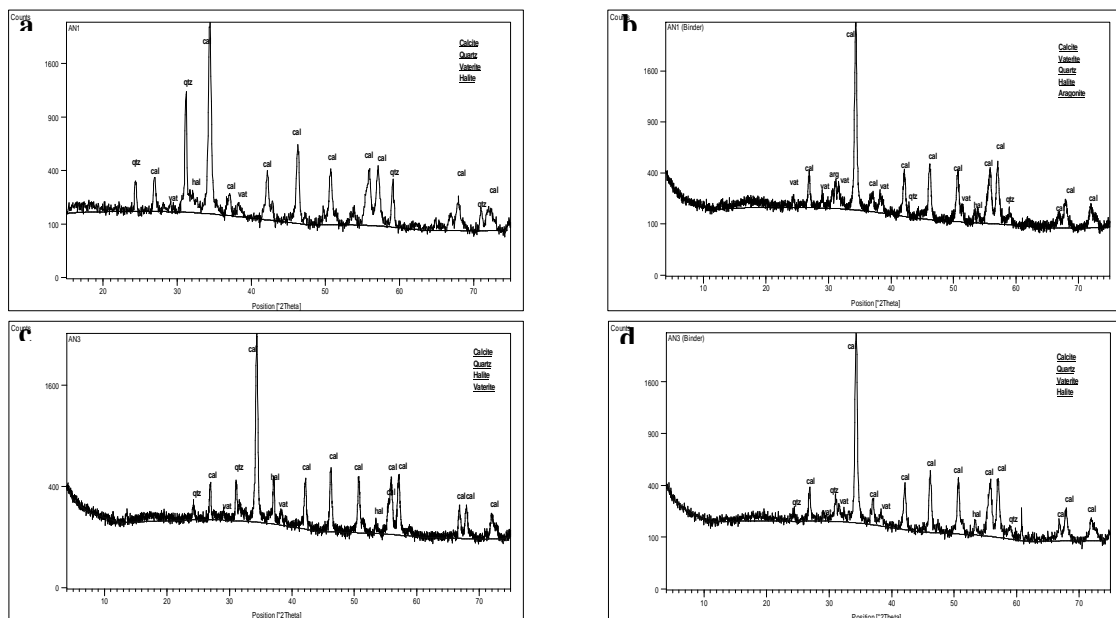


Figure (5) Shows XRD pattern of AN1 samples **a.** bulk sample, **b.** fractions rich in binder & AN3 samples, **c.** bulk sample, **d.** fractions rich in binder.

### 3.4. SEM/EDX Results

SEM/EDX observations of three mortars from Loom Factory site revealed various composition of a binder. Calcium is its main component, however aluminum and silicon occur in minor amounts, fig.

(6-a, b) especially in samples AN1 and AN2 respectively. Some samples (mainly AN3 from one of the loom pits) exhibit high content of sodium and chloride, fig. (6-c).

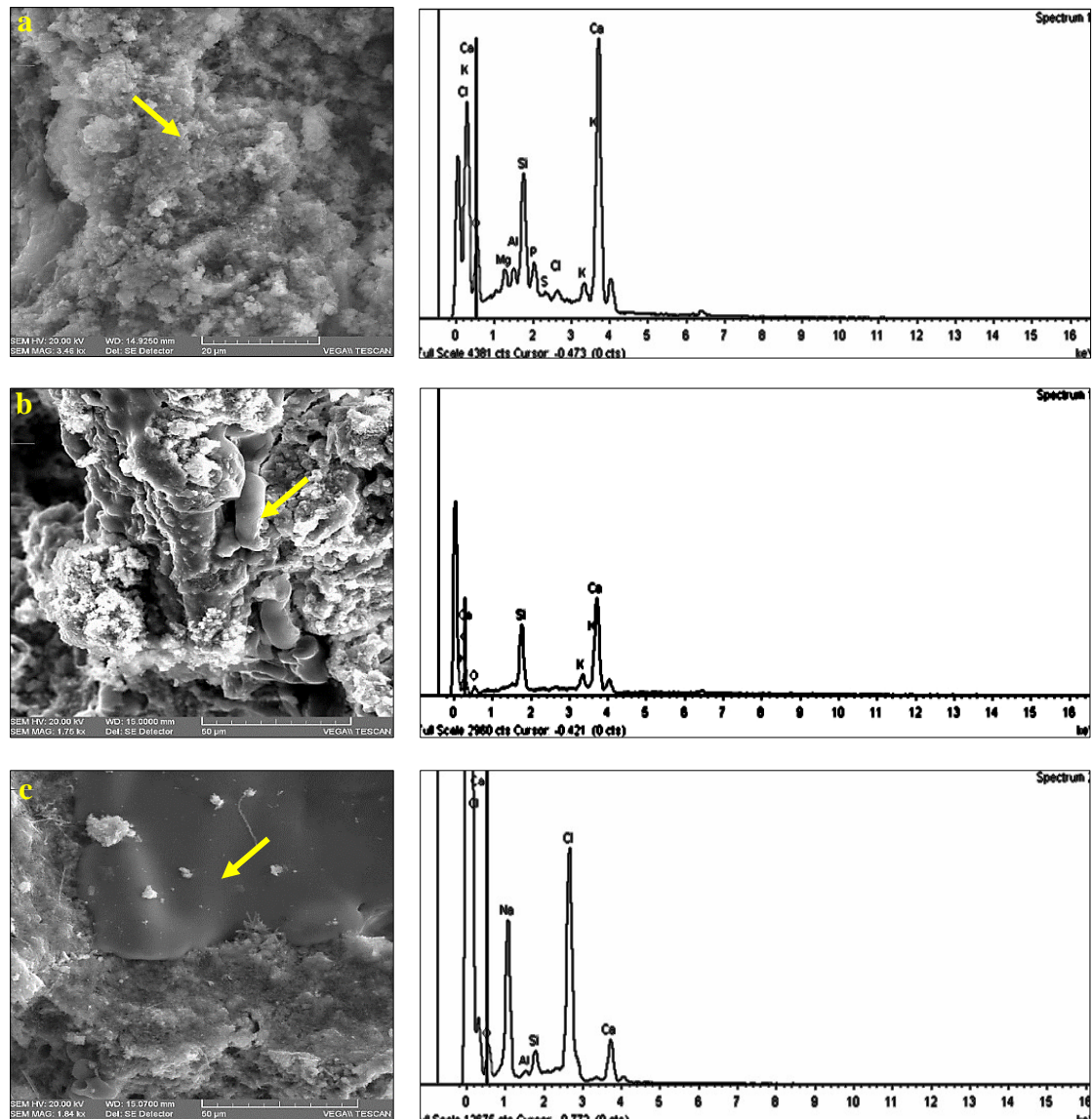


Figure (6) Shows SEM Microphotograph and EDX a. analysis for sample AN1 bulk sample, b. analysis for sample AN2, c. analysis for sample AN3

### 3.5. Results of acid attack

Results of acid attack for Loom Factory samples were almost similar at all levels, tab. (2). Percentages of insoluble aggregates are identical and lower than 50 %. They were as follows: 29.55 % for (AN1), 27.83 % for (AN2), 28.68 % for (AN3) and 29.14 % for (AN4). Percentages of carbonates contents range from 48.89 % to 52.30 %. Soluble

fractions are relatively high ranging from minimum 18.56 % to maximum 24.97 %. As for cementation index ( $C_i$ ), all samples are below 0.15. Binder/aggregate ratios revealed similarity of samples AN2, AN3, AN4 with binder/aggregate ratio close to 1.8:1 and relatively lower ratio (1.5:1) in sample AN1.

Table (2) Percentages of siliceous aggregates, carbonates, soluble fraction, cementation index, and binder/aggregate (b/a) ratios.

Sample	Carbonates %	Insoluble aggregates %	Soluble fractions %	Cementation Index (CI)	B/A ratio
AN1	48.89	29.55	24.97	0.10	1.5 : 1
AN2	50.03	27.83	21.89	0.10	1.8 : 1
AN3	52.30	28.68	19.02	0.09	1.8 : 1
AN4	52.30	29.14	18.56	0.09	1.8 : 1

### 3.6. Results of AAS and Colorimetry

Results of AAS and Colorimetry, tab. (3-a, b) revealed relatively high percentages of chloride (Cl) in all sam-

ples, reaching the maximum values in samples AN1 and AN2 (1.25 % and 1.28 % respectively).

Table (3-a) Results of chemical analysis of elements samples by AAS (converted to oxides)

Sample	Concentration %								
	SiO <sub>2</sub>	Ca O	Fe <sub>2</sub> O <sub>3</sub>	AL <sub>2</sub> O <sub>3</sub>	MgO	MnO	Na <sub>2</sub> O	K <sub>2</sub> O	TiO <sub>2</sub>
AN1	0.61	34.19	0.73	1.26	1.140	0.03	0.51	0.54	0.03
AN2	0.74	34.98	0.69	1.11	1.063	0.04	0.59	0.56	0.02
AN3	0.59	36.19	0.69	1.2	1.204	0.03	0.49	0.42	0.02
AN4	0.55	38.19	0.93	1.19	1.910	0.03	0.47	0.45	0.02

Table (3-b) Results of chemical analysis of samples by Colorimetry

Sample	Concentration measured by Colorimetry	
	SO <sub>3</sub>	Cl
AN1	1.34	1.25
AN2	1.54	1.28
AN3	1.31	0.63
AN4	1.39	0.70

### 3.7. Results of thermal analysis

The results of this technique reveal similar patterns of DTA/TG curves. Sample AN1 (the southern wall) reveals endothermic peak at 121.3 °C related to possible presence of secondary salts (gypsum). Carbonates show distinctive endothermic inflections at 629.3 °C and 837.5 °C, fig. (7-a). Sample AN2, fig. (7-b) (the western wall) shows two endothermic peaks at 108.8 °C, followed by 143.6 °C referring to presence of secondary product (double step dehydration of gypsum). Decomposition of carbonates was recorded at

638.3 °C. Sample AN3, fig. (7-b) (the first loom pit) has also two endothermic peaks, the first at 142.7 °C indicating presence of possible secondary products, and at 631.2 °C corresponding to the release of CO<sub>2</sub> from calcium carbonates. Sample AN4 (the second loom pit) has DTA/TG curves similar to sample AN3, with two endothermic peaks at 143.7 °C and 643.9 °C, fig. (7-d). All samples have similar total weight losses and very close percentages of carbonates contents as presented in tab. (4).

Table (4) Weight loss per temperature range for mortars from Loom Factory site

Sample	Weight loss per temperature range %				Carbonates %
	0-200 °C	200-600 °C	600-900 °C	Total weight loss %	
AN1	2.00	7.16	21.49	30.65	48.89
AN2	3.10	7.47	22.00	32.57	50.03
AN3	1.10	7.72	22.90	31.72	52.30
AN4	2.00	6.26	22.90	31.16	52.30

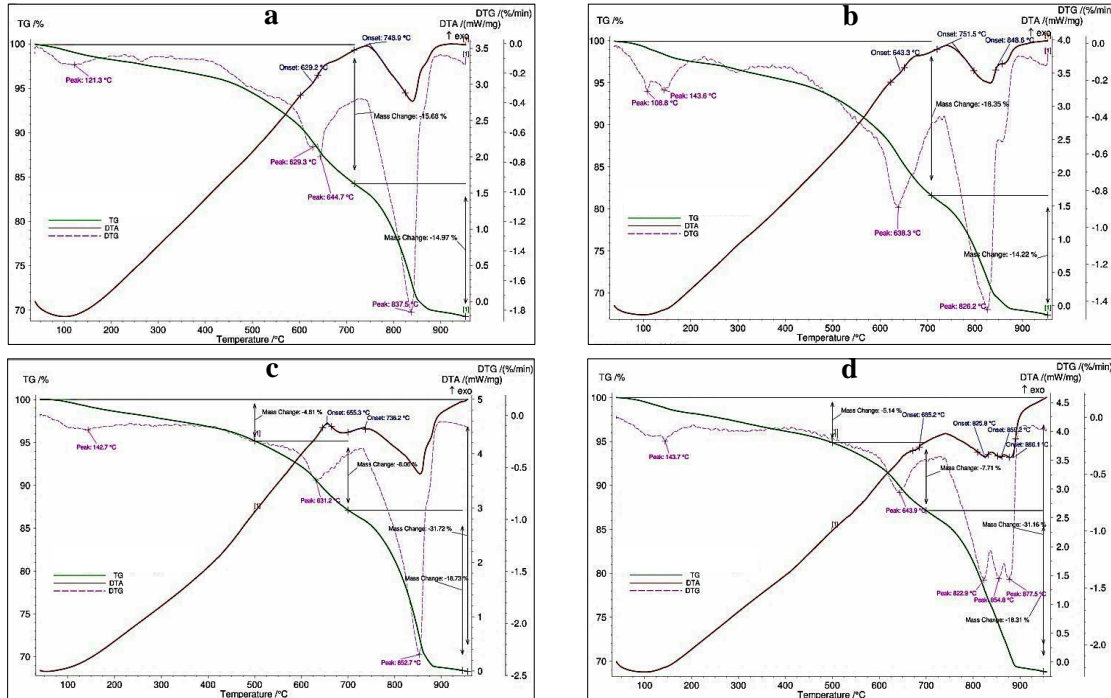


Figure (7) Shows DTA and TG curves of samples **a.** AN1, **b.** AN2, **c.** AN3, **d.** AN4.

### 3.8. Results of physical properties tests

The results of these tests are relatively similar. Density values for all samples are very close representing 1.21, 1.27, 1.30 and 1.24 g/cm<sup>3</sup> for samples AN1, AN2, AN3 and AN4 respectively. As for porosity measurement,

the results of all samples ranged from the minimum 34.1 % of sample AN1 (the southern wall of the Loom Factory) to the maximum 42.7 % of sample AN4 that belongs to loom pit. These measurements are presented in tab (5).

Table (5) Physical and mechanical measurements of Loom Factory site.

Sample	Location	Density g/cm <sup>3</sup>	Water content %	Porosity %	Compressive Strength (MPa)
AN1	Southern wall	1.21	3.47	34.1	-
AN2	Western wall	1.27	3.05	39.03	1.72
AN3	1 <sup>st</sup> loom pit	1.30	2.89	34.22	1.83
AN4	2 <sup>nd</sup> loom pit	1.24	3.46	42.7	-

Grain size distribution results, fig. (8-a) have revealed that mortar samples of Loom Factory have similar distribution of grain size. The most abundant fraction proportion for all samples is 0.5 mm with percentages

23.10 %, 26.19 %, 24.14 % and 25.49 % for samples AN1, AN2, AN3 and AN4 respectively. Cumulative curves for all samples from Loom Factory site are almost identical, fig. (8-b).

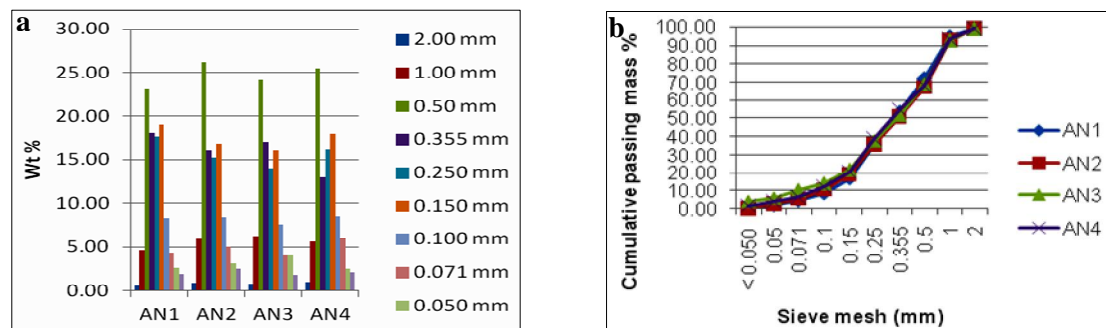


Figure (8) Shows **a.** Grain size distribution of mortar samples, **b.** Cumulative percentage curve for mortar samples.

#### 4. Discussion

All samples from Loom Factory present similar characteristics when examined by naked eye, stereomicroscope, and further analysis. Similarities between different samples in terms of physical, chemical, and mineralogical characteristics which are rather typical as in sieving analysis suggest that the whole building has been erected during single construction phase without further modifications. The petrographic feature of abundant lime lumps inclusions in combination with their big size, may point to non-sufficient calcination process, or imply a hot lime mixing technology/dry slaking method [15]. This observation leads to the conclusion of dealing with material of low quality and technology. Since in the Loom Factory there is rather limited need for water to be used, except perhaps for cleaning purposes, the observed abundant amount of charcoal may indicate rather impurities coming from a kiln (remnants of its fuel) together with burned lime but not intentional use, to modify mortar properties. Based on petrographical characteristics, all samples have similar mineralogical composition of the filler. This indicates the same source of raw material for the filler of all samples, belonging to single building phase. Presence of lime associated with organic matter, ranging from fresh pieces to typical charcoals in samples AN1 and AN3 indicates to relationship between presence of those various organic matters and the appearance of vaterite phase. That is reported in literature, that vaterite may develop with time in a hot climate enhanced by the presence of combustion gases [16]. In addition, it was mentioned that it can be associated with the presence of the organic compounds, which were added to the mixture, and their degradation products as in stucco used in Saint Peter basilica in Rome [17]. Their presence (i.e. organic compounds)

may lead to changes in other properties, specifically, larger distribution of pore size [18]. The presence of aragonite, detected by means of XRD, could be a result of the occurrence of bioclasts (shells of mollusc or brachiopod). These shells could be one of the components of the aggregates, used as filler. Furthermore, both aragonite and vaterite could result from presence of furnace slag [18]. Some of those features and conditions may apply to our case, specifically the presence of various organic matter and relatively hot climate. Detecting of halite NaCl and observing its relative high values refers to that site was affected by salt (chlorides) crystallization. As for cementation index ( $C_i$ ), all samples are below 0.15 referring to using pure lime. Binder amount, which is higher than amount of aggregates, refers to abundant use of lime, which in turn may refer to be obtained from near local quarry at the west bank of the Nile. That similarity in the results of the thermal analysis stands in good agreement with similarity in results of other kinds of analysis of sample from Loom Factory, confirming use of the same materials, and pointing to one phase of construction. According to the weight losses of samples at certain temperature range 600 °C - 900 °C, it can be concluded that contents of carbonates in all mortars are close to or equal 50 %. That indicates using high amount of lime in preparation of mortars. Similarity between all samples in terms of density and porosity and grain size distribution leads to similar results of compressive strength tests, suggesting the possibility of using the same composition of mortar for head and bed joints with no later amendments. The relatively low values of compressive strength for tested samples present rather weak state of preservation.

## 5. Conclusions

The present study contributed with some observations, which may help in analysis of building structure, specifically its chronology. Since all samples from Loom Factory site near Sohag presented similar characteristics in terms of composition and manufacturing procedures, they are possibly pointing to the fact that all the samples belong to one building phase using the same source of materials. This work reveals significant aspect related to damage represented by crystallization of salts which affects not only the mortar, but also the surrounding building materials (red bricks and plasters). Gathered data of various characteristics have led to documentation of its composition, technology, and damage aspects to composition of mortar and its state of preservation as well as helping as a guide for further conservation works.

## References

- [1] Farag, R., (1983). Excavations at Abydos in 1977: A Byzantine loom factory, *Mitteilungen des Deutschen Archäologischen Instituts Abteilung Kairo*, Vol. 39, pp: 51-57.
- [2] Ball, J., (2009). The missing link: Filling the gap in the evolution of medieval domestic looms, in: Alchermes, J., Evans, H. & Thomas, T. (eds.) *Αναθήματα Εορτικά: Studies in Honor of Thomas F. Mathews*, Mainz, pp: 40-46.
- [3] Leslie, A. & Eden, M., (2008). *A code of practice for the petrographic examination of mortars, plasters, renders and related materials*, Technical report, Applied Petrography Group, UK.
- [4] Bakolas, A., Biscontin, G., Contardi, V., Franceschi, E., Moropoulou, A., Palazzi, D. & Zendri, E. (1995). Thermo analytical research on traditional mortars in Venice, *Thermochim ACTA*, Vol. 269, pp: 817-828.
- [5] Moropoulou, A., Bakolas, A. & Bisbikou, K. (2000). Investigation of the technology of historic mortars, *J. of Cultural Heritage*, Vol. 1(1), pp: 45-58.
- [6] Middendorf, B., Hughes, J., Callebaut, K., Baronio, G. & Papayianni, I. (2005). Investigative methods for the characterisation of historic mortars-Part 1: Mineralogical characterization, *Materials and Structures*, Vol. 38, pp: 761-769.
- [7] Middendorf, B., Hughes, J., Callebaut, K., Baronio, G., & Papayianni, I., (2005). Investigative methods for the characterisation of historic mortars-Part 2: Chemical characterisation, *Materials and Structures*, Vol. 38, pp: 771-780.
- [8] Callebaut, K., Elsen, J., Van Balen, K. & Viaene, W., (2001). Nineteenth century hydraulic restoration mortars in the Saint Michael's Church (Leuven, Belgium) natural hydraulic lime or cement?, *Cement and Concrete Research*, Vol. 31, pp: 397-403.
- [9] Middendorf, B., Baronio, G., Callebaut, K., Hughes, J., (2000). Chemical-mineralogical and investigations of old mortars. In: RILEM (ed.) *Proceedings of an International Workshop Historic Mortars: Characteristics and Tests*. Paisley, pp: 53-61.
- [10] Wyrwicki, R., (1988). *Analiza derwywotograficzna skał ilastych*, Wydawnictwo Uniwersytetu Warszawskiego, Warszawa.
- [11] Thomson, M., Lindqvist J. E., Elsen J. & Groot C., (2004). Porosity of historic mortars, Martens, D. & Vermeltfoort, A. (eds.) *In 13<sup>th</sup> Int. Brick and Block Masonry Conference*, Amsterdam, pp: 1-10
- [12] Osman, A., Bartz, W., Kosciuk, J., (2014), Characterization of binding lime mortar used in the Anba Bishoi Monastery near to Sohag, (Egypt), pre-print in: IMS (ed.), *9<sup>th</sup> international masonry conference (9IMC)* Portugal, pp: 1-12.
- [13] Válek, J. & Veiga, R., (2005), Characterisation of mechanical properties of historic mortars: Testing of irregular samples, in: Brebbia, C., Wessex Institute of Technology & Torpiano, A. (eds.) *Structural Studies*,

- Repairs and Maintenance of Heritage Architecture IX, Transactions on the built environment*, pp:365-374.
- [14] Sassoni, E., Franzoni, E., & Mazzotti, C., (2015), Influence of sample thickness and capping on characterization of bedding mortars from historic masonries by double punch test (DPT), *Key Engineering Materials*, Vol. 624, pp: 322-329.
- [15] Hughes, J., Leslie, A. & Callebaut, K., (2001). The petrography of lime inclusions in historic lime based mortars, *Annales Geologiques des pays Helleniques*, Volume XXXIX, pp: 359-364.
- [16] Signorelli, S., Peroni, C., Camaiti, M. & Fratin, F., (1996). The presence of vaterite in bonding mortars of marble inlays from Florence Cathedral, *Mineralogical Magazine*, Vol. 60, pp: 663-665.
- [17] Fiori, C., Vandini, M., Prati, S. & Chiavari, G., (2009). Vaterite in the mortars of a mosaic in the Saint Peter basilica, Vatican (Rome), *J. of Cultural Heritage*, Vol. 10, pp: 248-257.
- [18] Wowra, O., (2002). Effects of carbonation to microstructure and pore solution, in Pro 24, in: Setzer M., Auberg, R. & Keck, H. (eds.) *Int. RILEM workshop on frost resistance of concrete from nanostructure and pore solution to macroscopic behavior and testing*, pp:61-68